forum acusticum 2023

SIMULATION-BASED DESIGN STRATEGY AND EXPERIMENTAL VALIDATION OF AN ACTIVE NOISE CONTROL SETUP

Maximilian Budnik, Valentin Mees
Fraunhofer Institute for Structural Durability and System Reliability LBF, Darmstadt, Germany

ABSTRACT

During the pandemic, mobile ventilation systems became increasingly popular. These systems filter the air in a room by moving it through a filtration system. This process generates noise, primarily at the air inlet and outlet of the unit. To meet regulatory requirements and design goals this noise must be minimized. Active Noise Control (ANC) is an effective way to influence airborne sound paths. To mitigate broadband stochastic noise, reference microphones within the ventilation system detect the noise in advance. By using an array of multiple loudspeakers, the propagation of noise into the free field can be controlled. Such an ANC system can also reduce noise in many other applications, such as heat pumps, industrial ventilation, and residential air conditioning. Setting up an acoustic simulation model and a virtual test bench can significantly increase design efficiency. This improves the quality of the solution in advance without relying on a physical prototype. Such a setup allows for efficient numerical investigations on appropriate positioning of ANC components, how to parameterize the controller, and what to expect in the real world. Free-field simulations are performed using the finite element (FE) method and transferred to a time-domain system simulation to evaluate component placement and controller design.

Keywords: *Simulation, Active Noise Control, Control Optimization, Validation*

**Corresponding author*: *maximilian.budnik@lbf.fraunhofer.de.*

1. INTRODUCTION

Noise control and design are becoming increasingly important in a growing number of applications, especially in residential environments. One application that has become very popular during the pandemic is mobile ventilation systems. In mobile ventilation systems, the top opening is the main noise outlet. Therefore, this opening is well suited for Active Noise Control (ANC). ANC can reduce lower frequencies better than passive attenuation measures of comparable size. In such a system, the sound and spectral content of the radiated broadband noise varies with the set airflow rate. Therefore, optimal noise reduction cannot be achieved with static narrow-band solutions such as Helmholtz resonators. Here, adaptive ANC enables compact solutions for non-stationary noise sources.

Active acoustic attenuation measures are often designed directly on the physical radiating object as a subsequent process. In a previous article [1], the authors presented a simulation-based approach where instead a simulation model is created first. This allows acoustic measures to be efficiently developed and evaluated in early design stages. The same article also describes how to build an efficient and valid numerical simulation model - the same model is used for the investigations described in this contribution.

ANC is an effective way to influence airborne sound paths, following the scheme shown in Fig. 1. The main concept with the loudspeaker characteristics and the array layout itself is constrained in the presented case by the outlet geometry and the target frequency range from 100 Hz to 800 Hz and the corresponding one-third octave bands. However, the number and position of each reference and error microphone or sensor are subject to optimization. The positioning of the error sensors will drive the investigation as it is strongly related to the overall goal of reducing the total radiated sound power.

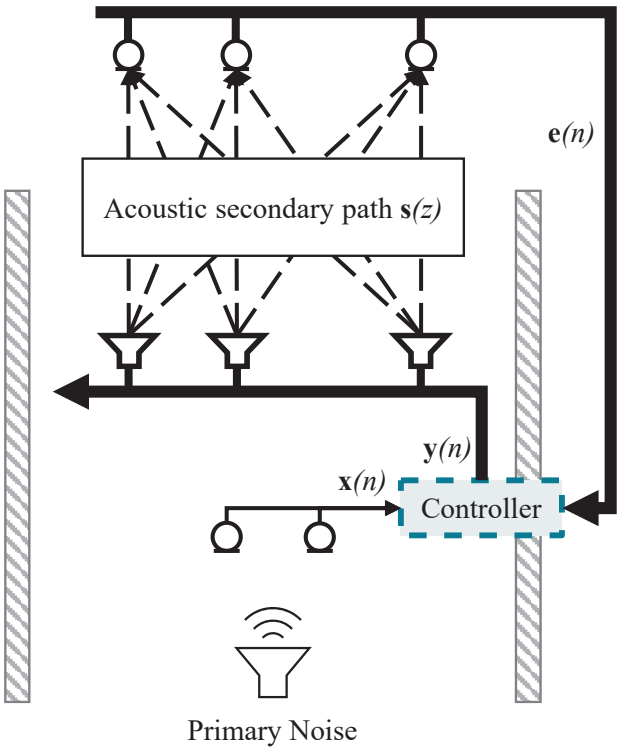

Figure 1. MIMO ANC System in an open box or duct, after [2]

In [3], the well-known Freqeuncy Response Assurance Criterion (FRAC) [4] was used as an evaluation metric that relates the reference and error positions. In this work, the radiation surface given by the outlet geometry is used to optimize the position of the error microphones in the error sensor plane with respect to the total radiated sound power and to find reference microphone positions where the frequency response function (FRF) is as highly correlated as possible with the error sensors. In this process, harmonic simulations are performed using the Finite Element Method (FEM) to evaluate the optimal sensor positioning. Subsequently, transient simulations are performed to characterize the acoustic system (impulse responses) and to obtain transfer functions between predetermined (loudspeakers) and previously found (sensors) locations in the system.

The transfer functions are used to construct a reduced system model that includes only the most important points and the acoustic paths between them. Matching simulation and experiment as early as possible, as described in [1], provides the basis for a reliable design process.

1.1 Adaptive MIMO ANC

The concept of ANC was first introduced in the 1930s by Paul Lueg, who attempted to cancel noise in an airplane cockpit using a microphone and a loudspeaker [5]. However, the first practical implementations of ANC were demonstrated in the 1980s.

Since then, there have been numerous developments in the field of adaptive ANC, with researchers continually improving the algorithms used to reduce noise and expanding the range of applications for the technology. Today, ANC is well established in headphones and automobiles, with effects limited to enclosed spaces. Although theoretically well understood and described, e.g. in [6] and [7], practical applications of ANC for free-field radiation are still rare due to the more complex calculations and more extensive loudspeaker configurations required.

MIMO (Multiple Input Multiple Output) ANC is a type of active noise control that uses multiple microphones and loudspeakers to create a sound field that cancels out the unwanted noise radiating from a given source. In this technique, multiple microphones are placed around the source to measure the noise being emitted. The signals from these microphones are then used to generate an anti-noise signal that is fed into multiple loudspeakers placed around the source. The anti-noise signal is designed to cancel out the noise that is being emitted by the source, thus reducing the amount of noise that is radiated into the open space.

The idea of adaptive ANC, which involves continuously updating the anti-noise signal based on the measured noise signals, was first proposed by Robert J. McAulay and Marilyn L. Malpass in 1980. They published a paper entitled ”Speech Enhancement Using a Soft-Decision Noise Suppression Filter” [8], which introduced the concept of adaptive filtering for noise reduction. This paper is considered to be the foundation of the modern techniques of adaptive noise reduction. The adaptation algorithm uses a set of mathematical equations to determine the optimal anti-noise signal that will cancel the noise signal. The adaptation algorithm takes into account the frequency content and spatial characteristics of the noise signal and adjusts the anti-noise signal to achieve maximum cancellation.

Overall, adaptive MIMO ANC is an effective technique for reducing noise radiation into the free space. It can be used in a variety of applications, including noise reduction for industrial equipment, transportation systems, and wind turbines.

1.2 Measuring acoustic simulation quality - KPI

When implementing numerical simulation models, there are several critical quality criteria or Key Performance Indicators (KPIs) that must be considered to ensure the accuracy, reliability, and effectiveness of numerical simulation models. With respect to an ANC system, the **phase and magnitude response** of the simulation model should be accurate and consistent with the actual behavior. This is important because it affects the systems ability to detect and control unwanted noise. Group delay, as a derivative of phase, is an intuitive measure of the time delay that occurs between an input and an output. The delay introduced by digital signal processing can be well approximated. A simulation model with realistic **group delay** is desirable because it can be used to optimize microphone placement and give an indication of how much additional delay can be introduced. The simulation model should also be **computationally efficient** and able to produce results in a reasonable amount of time. This is important because complex simulation models with high computational requirements are impractical for iterative optimization. Whenever possible, the simulation model should be **validated** against experimental data to ensure that they accurately represents real-world behavior. In addition, a **sensitivity analysis** can be performed to evaluate the effect of input parameters on the output of the simulation model. This analysis helps to identify critical parameters that affect performance and can be used to optimize the design and operation of the system.

Two stages can be distinguished: the physics-based FE analysis (FEA) and the Rapid Control Prototyping (RCP) for the design and parameterization of the ANC system. In the first step (FEA), the physics must be accurately modeled to numerically evaluate and analyze the sound propagation in fluids or air as a medium and to obtain valid data for control simulation. The second step (RCP) uses the FEA results (reduced system model of transfer functions). This step can then be used to design and parameterize the system and predict the effectiveness of the ANC system. Some of the KPIs are directly related to the validity of the physical simulation model and should therefore be investigated as part of the FEA. One such KPI is the accuracy of the amplitude and phase response in the simulation, which can be evaluated by comparing the transfer characteristic between the simulation and experimental data. Simulation efficiency on the other hand is related to the second stage and should be evaluated during RCP.

2. DEMONSTRATOR

To illustrate the process, a simplified mobile ventilation system is chosen as a demonstration example. The abstraction levels are shown in Fig. 2. The demonstrator is a wooden box with the dimensions of a mobile ventilation system (1), with an array of secondary sources (2), and a simplified loudspeaker excitation (3). The airborne sound path dominates the radiation pattern of this system, making it an ideal candidate for an ANC system. By using a suitable active concept, it is possible to intervene directly in the airborne sound path without significantly affecting the airflow by passive measures. Low-frequency radiation from the opening is approximately spherical, which could be compensated for with a single loudspeaker. However, since in the real system the noise does not originate from a discrete location, but is a combination of fan and flow noise, no single loudspeaker can be positioned close to the source. Therefore, the wavefront must be replicated over a larger area using multiple loudspeakers. At higher frequencies, the directivity also increases and sound lobes are formed [9]. To reproduce these secondarily (beam forming), several loudspeakers are required.

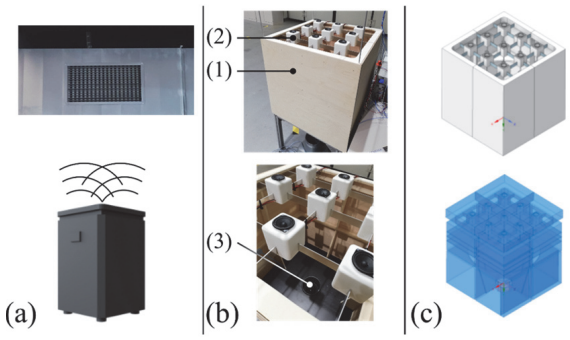

Figure 2. Demonstrator levels: (a) Typical ventilation systems [10]; (b) Physical demonstrator; (c) CAD model and acoustic model of the demonstrator.

2.1 Modelling

The FE model, shown in Fig. 3, is based on the computer-aided design (CAD) geometry of the simplified ventilation system, including the loudspeaker array described below. The FE model is a pure acoustic model: no fluid-structure-interactions are considered, only the air inside the box and a radiation region to avoid reflections. Since the model is symmetric, only a quarter of it is necessary.

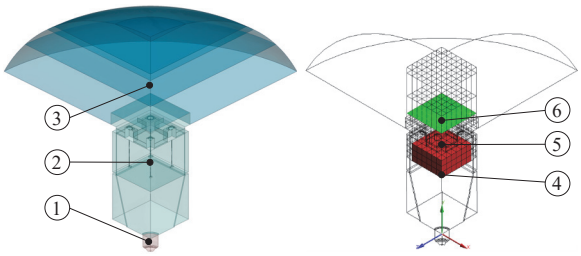

Figure 3. Acoustic simulation model: excitation (1), interior (2), radiation space (3), reference microphones (4), secondary sources (5), error microphones (6).

The secondary loudspeakers are distributed across the top opening of the demonstrator. They should be positioned so that no higher order spatial harmonics can propagate in the target frequency range, which is equivalent to avoiding side lobes [11, 12].

Depending on the angle of incidence θ, the first higher order spatial harmonic can radiate above

$$f_c = \frac{c}{d(1 + |\sin\theta|)} \tag{1}$$

as derived in [12]. For normal incidence, this reduces to $f_c = \frac{c}{d}$. For design, the extremal case of $\theta_{max} \approx 90°$ is considered. A speaker distance $d = 200\,\mathrm{mm}$ is chosen, allowing for theoretical ANC up to $920\,\mathrm{Hz}$. In the test setup, the noise originates at the bottom center of a square box with edge length $740\,\mathrm{mm}$ and height $840\,\mathrm{mm}$ which is completely open at the top. Therefore, considering a single wall reflection, the maximum incidence angle can be estimated to be $\theta_{max} \approx 50°$.

The loudspeaker excitation in the FEA is realized by applying a velocity excitation to the diaphragm of the modeled loudspeaker, as shown in Fig. 4. If only this is considered, the radiation characteristics are frequency independent and only influenced by the circular diaphragm shape. However, real loudspeakers exhibit frequency-dependent behavior caused by the electrodynamic loudspeaker characteristics. Therefore, it is necessary to determine the transfer function of the loudspeaker in its enclosure and include it in the simulation results. This can be done analytically using a lumped parameter model (Fig. 4) and is described analytically in [13, 14]. Using this approach, a numerically efficient and valid simulation model can be established for data extraction without the need for a physical demonstrator [1].

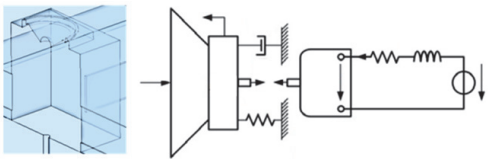

Figure 4. Left: Loudspeaker enclosing geometry of a secondary source. Right: Lumped-parameter model for the analytical description of the transfer behavior of a loudspeaker in a housing, after [14]

To design an effective ANC controller, system identifications are necessary. Typically, a broadband signal is applied in experiments, and the response is measured at the microphones. In FEA, simulations in the frequency domain or transient simulations can be performed, e.g. with harmonic, noise or pulse excitation. Time-domain simulations have the advantage of modeling transient processes and allow for the direct use of the obtained impulse responses in the RCP design process. To verify the simulation approach, a validation for an initial setup is provided. The results from simulation and experiment are compared by transforming the transient results into the frequency domain. Fig. 5 illustrates this comparison for the transfer function from the primary excitation to an exemplary reference microphone. The results show good agreement between experiment and simulation, both in terms of characteristics and level, although the phase response simulatively shows a slightly lower group delay.

After extracting the system identifications and establishing a RCP, an initial ANC concept can be evaluated. Fig. 6 shows this for an initial setup where the reference microphones were placed centrally $150\,\mathrm{mm}$ below the secondary sources and the error microphones $250\,\mathrm{mm}$ above. Fig. 7 shows the sound power level reduction at the error sensor locations averaged over one-third octave band. It is visible in both figures that the ANC concept works in the expected frequency range, but not uniformly over the entire frequency range. It can also be seen that there are only minor level reductions in the lower frequency regions where stronger effects should be possible. As shown in [3], this can result from reference sensors that are not optimally positioned. Since the reference sensors should be correlated with the error sensors, it is necessary to first determine the most reliable error sensor locations and then choose reference sensor positions related to them.

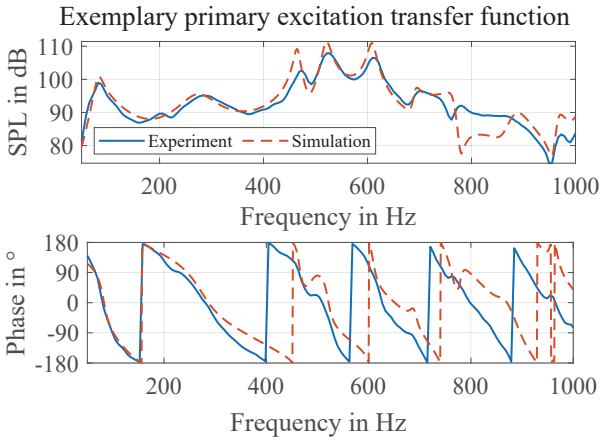

Figure 5. Comparison of an exemplary transfer function by magnitude and phase response between experiment and simulation for a primary excitation to an error sensor.

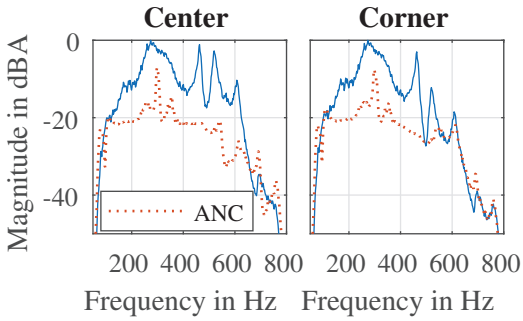

Figure 6. Initial ANC results for two sensors.

3. OPTIMIZATION PROCEDURE

Following the previous, the next step is to establish error microphone positions such that the radiated noise can be captured most effectively. There are three aspects to optimizing:

1. Positions should be highly correlated with the total radiated sound power over the frequency range, e.g., high intensity regions, and close enough to record primarily the target signal and not uncorrelated noise.

   Placing the error microphones in areas of high intensity increases the signal-to-noise ratio with respect to both external and recording noise. External noise is not considered in this paper, but as a rule of thumb, the microphones should be placed as close as possible as given by the second point. This decay distance has been derived in [12] as

   $$z = \frac{d \log 10}{\sqrt{(2\pi)^2 - (k_0 d)^2}} \tag{2}$$

   for a decay of 20 dB of the first harmonic.

2. Distances to secondary speakers must be high enough so that evanescent higher order spatial harmonics decayed by at least 20 dB. Based on the speaker spacing, the minimal required distance for the error microphones with a target frequency of 800 Hz is $\approx$ 8.5 cm. The search space for the error microphones is set to 10 cm above the speaker plane.

3. The final requirement is to capture a signal that best represents the total radiated sound power. Therefore, microphone placement must be chosen so that most of the radiated sound power is captured in the target frequency range.

Because the error plane is close to the edge of the box, a large fraction of the total radiated sound passes through the error plane, but the measured wave is not yet planar, i.e., the sound velocity and sound pressure are not in phase. Therefore, the error microphones cannot simply be placed at a grid spacing of $\lambda_{min}/2$. A suitable method

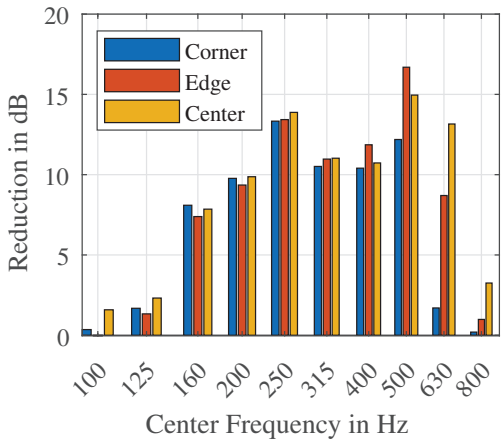

Figure 7. Simulated ANC reduction at error sensor positions averaged over one-third octave bands.

to indicate the sound power is the evaluation of Sound Intensity (SI) measurements with a corresponding "flowed through" area. However, SI measurements are cumbersome to perform and evaluate. Again, the validated simulation model has great strength. The sound power P is given by

$$P = \int \boldsymbol{I} d\boldsymbol{S} = \int p \boldsymbol{v} d\boldsymbol{S}, \tag{3}$$

which is the vectorial sound intensity $\boldsymbol{I}$ integrated over the normal component of the surface vector $\boldsymbol{S}$. The intensity can also be described by the pressure p multiplied by the normal component of the velocity vector $\boldsymbol{v}$. Using FEA, it is possible to evaluate the sound power over arbitrary shapes of enveloping surfaces because the vector components of the velocities are computed precisely. Using this approach, a panel contribution to the total radiated sound power can be evaluated. If this is further decomposed, it is possible to calculate the sound power contribution of each node in a panel using the corresponding area and normal vector component. The sound power contribution is evaluated for each frequency for each node in the set and normalized to the maximum for that frequency. Since the distributions change minimally over the frequency range, four dominant distributions are determined by evaluating the mean across the frequency bands. Fig. 8 shows the simulated intensity distribution in the four frequency bands, evaluated for the error plane at 100 mm above the secondary sources (as shown on the right in Fig. 3).

The results show that one microphone placed centrally above the opening can adequately cover a frequency range up to 500 Hz. This position is still dominant up to 700 Hz, where the corners of the box also become radiation areas. The corners become more dominant in the 700 Hz to 800 Hz frequency range, and remain so for higher frequencies. Beyond 800 Hz, additional locations at the edge centers show an increased contribution, while the center location becomes nearly negligible. Considering the target frequency range of 100 Hz to 800 Hz, the locations shown in Fig. 9 are chosen to capture most of the radiated sound power characteristics with the minimum number of sensors required.

Finally, the reference microphones can be placed. Three objectives must be met:

1. The signals should be highly correlated with the error signals.

   Although the simulation does not account for noise, some considerations about signal correlation can be made based on the magnitudes of the transfer functions. In [3], the FRAC was used to evaluate the correlation between possible reference sensor positions and fixed error sensor positions. The same approach is extended here.

2. The sensors should not be located at nodes of the spatial Eigenmodes of the box (to achieve 1.).

   Since the demonstrator has semi-free field characteristics, standing waves or Eigenmodes of the air volume inside the box have to be considered. In [3] it was shown that oscillation nodes can occur in interaction with the secondary source enclosures, positioning in those nodes should be avoided.

3. Distances to the loudspeaker plane must be large enough so that signal acquisition, signal processing, and loudspeaker dynamics combined are not slower than the sound traveling through the air.

   As shown, the sound power contribution clearly indicates relevant error sensor positions. However, since the reference data is needed chronologically before the secondary source signals are emitted, the delay between the reference and error sensors must be considered.

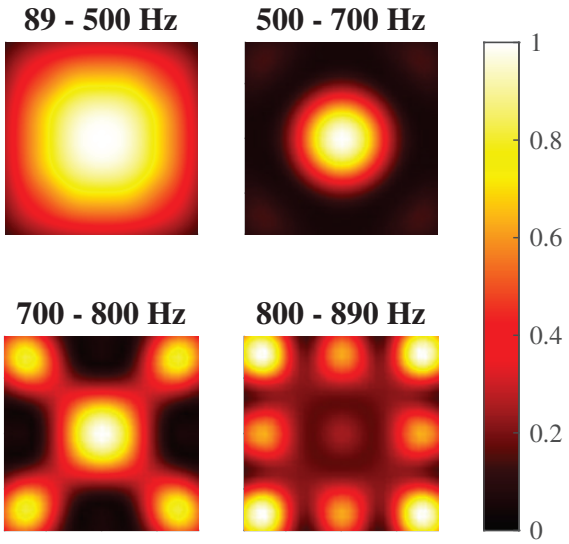

Figure 8. Normalized sound power contribution for possible error sensor positions. Averaged over frequencies with similar behavior. Top view with mirrored results of the quarter model.

The reference sensor positioning design space is created as shown in red on the right in Fig. 3. Each node within this space is compared to the error positions using the FRAC as a single value evaluation over the entire frequency range. The FRAC indicates three different reference sensor positions when symmetry conditions are neglected. All selected reference points are in the same xz-plane, which is as close as possible to the error plane in the design space. The resulting setup is shown in Fig. 9.

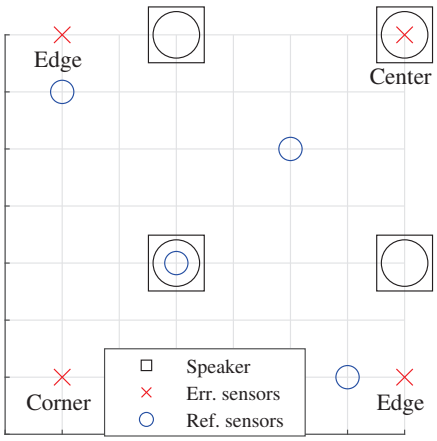

Figure 9. Top view of the quarter model with the arrangement strategy for the optimized ANC concept.

4. VERIFICATION OF DESIGNED SYSTEM

With the now fully determined ANC concept design, the RCP can be performed to predict the possible noise reduction. Fig. 10 shows the ANC effect with the new concept and Fig. 11 shows the corresponding sound power level reduction for the three error sensor locations averaged over one-third octave bands. As excitation, a noise signal measured on the real world reference system is used. The signal is concentrated in the frequency bands up to 630 Hz, with a gap around 400 Hz. In all high-amplitude bands, a reduction of at least 5 dB is achieved. The low-amplitude bands around 400 Hz and 800 Hz show only slight change, in the bands around 500 Hz and 630 Hz corner and center are well attenuated, but the error microphone at the edge of the box shows an increased amplitude. In summary, most of the targeted frequency ranges are well covered with strong and more constant noise reduction. When comparing the new results with the previous ones, the distances of the error levels also play an important role. At the previously higher distance of 250 mm, frequencies below 200 Hz are less dominant than at the new distance of 100 mm. Therefore, the first three considered bands show an improved reduction, while the higher frequency bands are considered less important by the algorithm.

To fundamentally compare the two results, a global measure of radiated sound power would be suitable. This can, e.g., be evaluated by replaying the simulated control signals in the FE simulation or using additional comfort points to calculate the radiated sound power according to a standard like DIN 3744 [15]. The RCP by itself cannot project the remaining excitation in the far-field. This would require the simulation of more transfer paths, e.g. to acquire samples on a closed surface with Nyquist-compliant cell sizes.

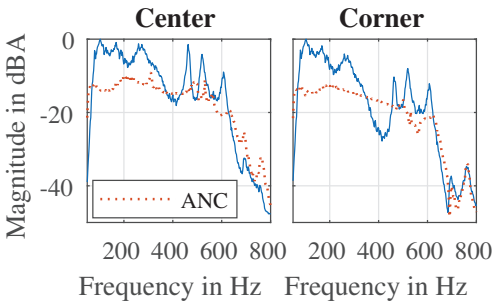

Figure 10. Top view of the quarter model with the arrangement strategy for the optimized ANC concept.

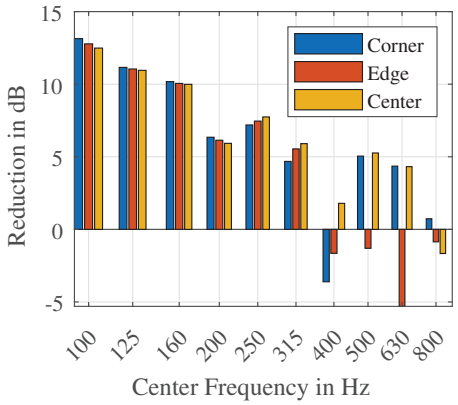

Figure 11. Simulated ANC reduction at error sensor positions averaged over one-third octave bands.

5. CONCLUSION AND OUTLOOK

The presented method allows the configuration of ANC measures through simulation-based design. The influence of the positioning of system components on the design of an ANC system for a semi-free-field application was shown and how simulations can be used for optimization. The sound power contribution investigation technique for the positioning of the error sensors and the FRAC-based optimization regarding the reference sensors allow global optimization. In future research, the power based optimization should be extended to a more detailed frequency specific optimization.

Further contributions will also include an approach to evaluate the resulting radiated sound power within the RCP or by replaying the simulated control signals in the FE simulation. Both methods require additional simulation time and have to evaluated regarding efficiency and result quality. In addition, FEA can visualize the resulting sound pressure distribution in space and thus the ANC effects.

The presented approach can be applied to a wide range of applications where active low-noise design and control are important. Hence, there is also a focus on the practical implementation with low-cost computing hardware, the necessary component design, and a detailed validation procedure.

6. REFERENCES

[1] M. Budnik and V. Mees, "Efficient simulative design, verification, and experimental validation of an active noise control measure for airborne sound radiation," in *Proc. of the Aachen Acoustics Colloquium*, (Aachen, Germany), pp. 159–168, 2022.

[2] B. Lam, D. Shi, W.-S. Gan, S. J. Elliott, and M. Nishimura, "Active control of broadband sound through the open aperture of a full-sized domestic window," *Scientific Reports*, vol. 10, no. 1, p. 10021, 2020.

[3] M. Budnik and V. Mees, "Simulationsbasierte Ermittlung der Anordnung von Mikrofonen und Lautsprechern bei aktivem Schallschutz," in *Fortschritte der Akustik - DAGA 2023*, (Hamburg, Germany), pp. 434–437, 2023.

[4] W. Heylen, S. Lammens, M. I. Friswell, and J. E. Mottershead, "FRAC: A Consistent Way of Comparing Frequency Response Functions," in *Proc. of the Conference on Identification in Engineering Systems*, (Swansea), pp. 48–57, University of Wales, 1996.

[5] D. Guicking, "On the invention of active noise control by Paul Lueg," *The Journal of the Acoustical Society of America*, vol. 87, pp. 2251–2254, 05 1990.

[6] S. M. Kuo and D. R. Morgan, *Active Noise Control Systems: Algorithms and DSP Implementations*. New York: John Wileys & Sons, 1996.

[7] C. H. Hansen, S. D. Snyder, X. Qiu, L. Brooks, and D. Moreau, *Active control of noise and vibration*. Boca Raton: CRC Press, second edition ed., 2020.

[8] R. McAulay and M. Malpass, "Speech enhancement using a soft-decision noise suppression filter," *IEEE Transactions on Acoustics, Speech, and Signal Processing*, vol. 28, no. 2, pp. 137–145, 1980.

[9] M. Möser, *Engineering Acoustics*. Berlin, Heidelberg: Springer Berlin Heidelberg, 2009.

[10] D. Beer, P. Fritzsche, B. Fiedler, J. Rohlfing, K. Bay, J. Troge, J. Millitzer, and C. Tamm, "Luftreinigungsgeräte – akustische Anforderungen und Optimierungsmöglichkeiten," in *Fortschritte der Akustik - DAGA 2022*, (Vienna, Austria), 2022.

[11] L. E. Kinsler, A. R. Frey, A. B. Coppens, and J. V. Sanders, *Fundamentals of acoustics*. New York and S.l.: Wiley and HathiTrust Digital Library, 4th ed. ed., 2000.

[12] S. J. Elliott, J. Cheer, L. Bhan, C. Shi, and W.-S. Gan, "A wavenumber approach to analysing the active control of plane waves with arrays of secondary sources," *Journal of Sound and Vibration*, vol. 419, pp. 405–419, 2018.

[13] E. Terhardt, *Akustische Kommunikation*. Berlin, Heidelberg: Springer Berlin Heidelberg, 1998.

[14] M. Rossi, *Audio*. Électricité, Lausanne and [Paris]: Presses polytechniques et universitaires romandes and [Diff. Géodif], op. 2007.

[15] "DIN EN ISO 3744:2011-02, Acoustics - Determination of sound power levels and sound energy levels of noise sources using sound pressure - Engineering methods for an essentially free field over a reflecting plane (ISO 3744:2010)."